Mathematical Modelling and Analysis
Volume 29, Issue 3, 426–441, 2024
https://doi.org/10.3846/mma.2024.19528

Mathematical Modelling Electrically Driven Free Shear Flows in a Duct under Uniform Magnetic Field

Harijs Kalis[a] **and Ilmars Kangro**[b]

[a] *Institute of Mathematics and Computer Science of University of Latvia*
Raina bulvāris 29, LV-1586 Rīga, Latvia
[b] *Institute of Engineering, Faculty of Engineering, Rezekne Academy of Technologies*
Atbrivosanas aleja 115, LV–4601 Rezekne, Latvia
E-mail(*corresp.*): ilmars.kangro@rta.lv
E-mail: harijs.kalis@lu.lv

Received July 19, 2023; accepted February 5, 2024

Abstract. We consider a mathematical model of two-dimensional electrically driven laminar free shear flows in a straight duct under action of an applied uniform homogeneous magnetic field. The mathematical approach is based on studies by J.C.R. Hunt and W.E. Williams [10], Yu. Kolesnikov and H. Kalis [22, 23]. We solve the system of stationary partial differential equations (PDEs) with two unknown functions of velocity U and induced magnetic field H. The flows are generated as a result of the interaction of injected electric current in liquid and the applied field using one or two couples of linear electrodes located on duct walls: three cases are considered. In dependence on direction of current injection and uniform magnetic field, the flows between the end walls are realized. Distributions of velocities and induced magnetic fields, electric current density in dependence on the Hartmann number Ha are studied. The solution of this problem is obtained analytically and numerically, using the Fourier series method and Matlab.

Keywords: magnetohydrodynamic (MHD) flow, Fourier series, PDEs system, electric current, Matlab solutions.

AMS Subject Classification: 35J57; 35J67; 35J25; 35J15; 35Q35; 35Q80; 65N22; 76W05; 76D99.

Copyright © 2024 The Author(s). Published by Vilnius Gediminas Technical University
This is an Open Access article distributed under the terms of the Creative Commons Attribution License (http://creativecommons.org/licenses/by/4.0/), which permits unrestricted use, distribution, and reproduction in any medium, provided the original author and source are credited.

1 Introduction

In many technological applications it is important to mix an electrically conducting liquid by using various magnetic fields. In [8] are used different external magnetic fields (homogeneous, radial, axial, dipolar) for mathematical modelling of 2-D MHD flow. In [7], distribution of electromagnetic fields, forces and temperature induced by the system of the alternating electric current in the conducting cylinder has been calculated.

The work [5] presents the mathematical model of metal electrodes of the form of bars placed parallel to the finite cylinder axis in the viscous incompressible liquid, these conductors are connected to the alternating current. In [6], the distributions of electromagnetic fields, forces and temperatures induced by 3-phase axially-symmetric system of electric current has been calculated; the MHD flow of viscous incompressible liquid is obtained by the finite-difference method. In [11,17], special monotonous difference schemes and averaging methods have been developed for solution of MHD problem of viscous incompressible fluids and for solving problems of mathematical physics.

In [23], a system of stationary partial differential equations with two unknown functions of velocity and induced magnetic field in the cylindrical coordinates is solved. In [19], a liquid with electrical conductivity and viscosity is in a cylindrical vessel with isolated walls and at the end wall $z = 0$ there is a pair of ideally conducting electrodes supplied with a current I, perpendicular to the plane $z = 0$. In [3], the laminar MHD flows with finite electrically conducting Hartmann walls are investigated using numerical simulations with OpenFOAM for Hartmann numbers $500 - 2000$.

In [4], the MHD flow of an incompressible conductive viscous fluid between two rigid planes (exact solution is obtained) is described. In [16], three types of flow – general 3-D flow, rotational flow and axi-symmetrix flow of a viscous incompressible conductive liquid in an induction-free approximation with external magnetic field parallel to z-axis are considered. The viscous electrically conducting incompressible liquid moves between infinite cylinders of square section placed periodically, the 2-D MHD flow around the cylinders an external uniform magnetic field are analysed in [14]. Similarly in [13], the liquid-electrolyte is to move between infinite cylinders placed periodically and the 2-D MHD convection around the cylinders are obtained.

Relevant simplified MHD equations in cylindrical coordinates in a non-dimensional form for an electrically driven flow were first used in [9, 10]. The coincidence of theoretical and experimental results was demonstrated in [9].

A mathematical model of 2-D electrically driven laminar axisymmetric circular free shear flows in a cylindrical vessel under the action of an applied axial uniform magnetic field was studied [23] (see Refs. there). The flows are generated as a result of the interaction of the electric current injected into the liquid and the applied field using one or two pairs of concentric ring electrodes located on the end walls. With growing Hartmann number, two lateral free shear layers and two Hartmann layers on the end walls are arising and between them a quasi-potential core is enclosed. Depending on the direction of current inflow, coinciding or two opposite flows are realized between the end walls.

Experiments with a rotating free shear layer in an axial magnetic field between two annular electrodes located on the end wall perpendicular to the magnetic field both for the steady regime in [21] were carried out. In [3], the transition flow laminar to time dependent MHD duct flows with finite electrically conducting Hartmann walls and isulating side walls is investigated. In [26], are provided data on the suppression of free surface instabilities of liquid metal film flows under the action of strong magnetic fields. In [2], numerical study of the induced electric current of electrovortex flow in a cuboid vessel is considered.

In the present article, we discuss steady-state laminar plane-parallel free shear flow of a viscous electrically conducting fluid in rectangular duct. This work is a continuation of an earlier physical study in MHD journal 1978-1984 [15,18,20] and 2021–2023 [12,22,23], where the flow in the duct was created by an electromagnetic force caused by the interaction of an electric current with an external uniform magnetic field. The electrically driven laminar plane free shear flows in a straight direct under the action of an applied uniform magnetic field with the angle ϕ_0 of inclination of the magnetic field vector B to these walls for $\phi_0 = \pi/2$ in [12] and for $\phi_0 = \pi/4$ in [22] are considered. In [18], the angle $\phi_0 = \pi/2$ only is considered. In these studies, the current was supplied to a pair of infinite linear electrodes on the duct wall perpendicular to the field.

In the present article for the mathematical modelling the flow is generated by an electromagnetic force associated by an external homogeneous magnetic field with its induction vector B directed at angles $\phi_0 = \pi/2$, $\phi_0 = \pi/4$ and $\phi_0 = 0$, with current supplied to a pair of infinite line electrodes on lower and upper wall of the duct.

2 Formulation of the problem

Following [25], the magnetohydrodynamic (MHD) flow is characterized by one non-dimensional parameter – Hartmann (Ha) number. The Hartmann number accounts for the strength of the applied magnetic field and, correspondingly, the value of the induced electric currents.

The MHD process is considered in duct cross section:

$$\Omega = \{(x, y, z) : -L \le x \le L, 0 \le y \le C, -\infty \le z \le +\infty\}$$

with electrically non conducting walls $x = \pm L, y{=}0; y{=}C$. External magnetic field in the (x, y) plane is applied as $\mathbf{B}{=}\{B_0 \cos(\phi_0), B_0 \sin(\phi_0), 0\}$, where B_0 is constant value of the magnetic field induction in the direction under angle ϕ_0.

An electric current is supplied to duct by two couples of linear electrodes $z \in (-\infty, +\infty)$ at $y = 0$ and $y = C$ by $x = -a, x = a$ on the duct walls perpendicular to the walls. At the walls $y = 0, y = C$ in the first electrode $x = -a$ the electric current densities $J_x = 0, J_y = +\infty$, in the second electrode $x = +a$ the electric current densities $J_x = 0, J_y = -\infty$.

Therefore, $J_y = \delta(x+a) - \delta(x-a)$. We will find the symmetric distribution of azymuthal velocity $U = U(x, y)$ and induced magnetic field $H = H(x, y)$

$\left(J_x = \frac{\partial H}{\partial y},\ J_y = -\frac{\partial H}{\partial x}\right)$ by solving the following first kind boundary value problem for two partial differential equations (PDEs) [10]:

$$\begin{cases} \frac{\partial^2 U}{\partial x^2} + \frac{\partial^2 U}{\partial y^2} + Ha(\cos(\phi_0)\frac{\partial H}{\partial x} + \sin(\phi_0)\frac{\partial H}{\partial y}) = 0, \\ \frac{\partial^2 H}{\partial x^2} + \frac{\partial^2 H}{\partial y^2} + Ha(\cos(\phi_0)\frac{\partial U}{\partial x} + \sin(\phi_0)\frac{\partial U}{\partial y}) = 0, \\ x \in (-L, L), y \in (0, C), U(\pm L, y) = H(\pm L, y) = U(x, 0) = 0, \\ U(x, C) = 0, \ \ H(x, 0) = H_0(x), H(x, C) = \gamma H_0(x), \end{cases} \tag{2.1}$$

where γ is the constant, $H_0(x)$ is the following function:

$$\begin{cases} H_0(x) = 0, x \in [-L, -a), x \in (a, L], \\ H_0(x) = -I_0, x \in [-a, a], \end{cases}$$

where I_0 characterized the value of the electric current, $I_0 = 1$. For Equations (2.1) we use transformation $S_\pm = H \pm U, U = \frac{S_+ - S_-}{2}, H = \frac{S_+ + S_-}{2}$. Then,

$$\begin{cases} \frac{\partial^2 S_+}{\partial x^2} + \frac{\partial^2 S_+}{\partial y^2} + Ha(\cos(\phi_0)\frac{\partial S_+}{\partial x} + \sin(\phi_0)\frac{\partial S_+}{\partial y}) = 0, \\ \frac{\partial^2 S_-}{\partial x^2} + \frac{\partial^2 S_-}{\partial y^2} - Ha(\cos(\phi_0)\frac{\partial S_-}{\partial x} + \sin(\phi_0)\frac{\partial S_-}{\partial y}) = 0, \\ x \in (-L, L), \ \ y \in (0, C), S_\pm(\pm L, y) = 0, \\ S_\pm(x, 0) = H_0(x), \ \ S_\pm(x, C) = \gamma H_0(x). \end{cases} \tag{2.2}$$

Using the transformation $S_\pm(x, y) = W_\pm(x, y)\exp(- \pm \alpha(f_0(x, y))$ we obtain following boundary value problem for two Poissons's type PDEs:

$$\begin{cases} \frac{\partial^2 W_\pm}{\partial x^2} + \frac{\partial^2 W_\pm}{\partial y^2} - \alpha^2 W_\pm = 0, \\ x \in (-L, L), y \in (0, C), \ \ W_\pm(\pm L, y) = 0, \\ W_\pm(x, 0) = H_0(x)\exp(\pm \alpha x \cos(\phi_0)), \\ W_\pm(x, C) = \gamma H_0(x)\exp(\pm \alpha f_0(x, C)), \end{cases} \tag{2.3}$$

where $f_0(x, y) = x\cos(\phi_0) + y\sin(\phi_0), \alpha = Ha/2$, $Ha = 2aB_0\sqrt{\frac{\sigma}{\eta}}$ is Hartmann number, σ, η are electrical conductivity and dynamic viscosity, B_0 magnetic field induction.

When $\gamma = 0$, the electric current is applied only by lower couple of electrodes at $y = 0$ and not applied by two upper electrodes at $y = C$. If $\gamma = -1$, then the electric current injected by upper couple of electrodes at $y = C$ flows in area between electrodes in the identical direction with current from the lower couple of electrodes at $y = 0$. If $\gamma = 1$, the electric current injected by upper couple of electrodes flows in area between electrodes in direction opposite to the current from lower electrodes (see Figures 1–3).

3 The problem solution

For problem (2.3) solution we use Fourier method.

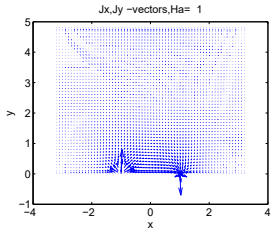

Figure 1. Electric current vectors Jx, Jy by $Ha = 1$ from $\gamma = 0$.

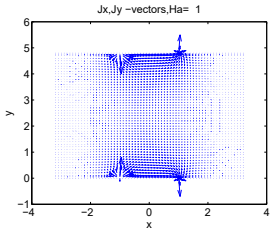

Figure 2. Electric current vectors Jx, Jy by $Ha = 1$ from $\gamma = -1$.

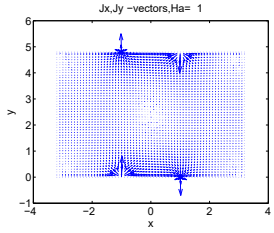

Figure 3. Electric current vectors Jx, Jy by $Ha = 1$ from $\gamma = 1$.

3.1 Fourier method for Equation 2.3

The Fourier series for function $f(x), x \in [-L, L], f(-L)=f(L)=0$ is in following form [1, 24]:

$$f(x) = \sum_{n=1}^{\infty} a_n X_n(x), \quad a_n = \frac{1}{L} \int_{-L}^{L} X_n(x) f(x) dx,$$

where $X_n = \sin(\lambda_n(x + L)), \lambda_n = \frac{n\pi}{2L}$, $\frac{d^2 X_n(x)}{dx^2} = -\lambda_n^2 X_n(x)$. Using Fourier series for functions $W_{\pm}(x, y)$ from(2.3) it follows: $W_{\pm}(x, y)=\sum_{n=1}^{\infty} X_n(x) Y_n^{\pm}(y)$, where $X_n(x), Y_n^{\pm}(y)$ are the separated values.

For homogenous PDEs from(2.3) it follows:

$$0 = \sum_{n=1}^{\infty} (-\beta_n^2 Y_n^{\pm}(y) + \frac{d^2 Y_n^{\pm}(y)}{dy^2}) X_n(x), \quad \beta_n = \sqrt{\alpha^2 + \lambda_n^2}.$$

The soluton of equation $-\beta_n^2 Y_n^{\pm} + \frac{d^2 Y_n^{\pm}(y)}{dy^2} = 0$ is given by

$$Y_n^{\pm}(y) = C_n^{\pm} \sinh(\beta_n y) + B_n^{\pm} \cosh(\beta_n y),$$

where $C_n^{\pm}, B_n^{\pm}$ are arbitrary constants. From boundary condition by $y = 0$ it follows :

$$H_0(x) \exp(\pm a_6 x) = \sum_{n=1}^{\infty} X_n(x) B_n^{\pm},$$

and

$$B_n^{\pm} = \frac{1}{L}\int_{-L}^{L} H_0(x)\exp(\pm a_6 x)X_n(x)dx$$
$$= -\frac{I_0}{L(\lambda_n^2+a_6^2)}(\exp(\pm a_6 a)(\pm a_{3,n}-a_{4,n}) - \exp(-\pm a_6 a)(\pm a_{1,n}-a_{2,n})),$$

where

$$a_6 = \alpha\cos(\phi_0),\quad a_{1,n} = a_6\sin(\lambda_n(L-a)),\quad a_{3,n} = a_6\sin(\lambda_n(L+a)),$$
$$a_{2,n} = \lambda_n\cos(\lambda_n(L-a)),\quad a_{4,n} = \lambda_n\cos(\lambda_n(L+a)).$$

We use following formulas [1]:

$$\int \exp(\pm a_6 t)\sin(\lambda_n t)dt = \frac{\exp(\pm a_6 t)}{a_6^2+\lambda_n^2}(\pm a_6\sin(\lambda_n t) - \lambda_n\cos(\lambda_n t)),\ t\in[-L,L]$$
$$\int \exp(\pm a_6 t)\sinh(\lambda_n t)dt = \frac{\exp(\pm a_6 t)}{a_6^2-\lambda_n^2}(\pm a_6\sinh(\lambda_n t) - \lambda_n\cosh(\lambda_n t)).$$

From boundary condition by $y = C$ follows:

$$\gamma H_0(x)\exp(\pm\alpha f_0(x,C)) = \sum_{n=1}^{\infty} X_n(x)Y_n^{\pm}(C)$$

and $C_n^{\pm}\sinh(\beta_n C) + B_n^{\pm}\cosh(\beta_n C) = \gamma\exp(\pm a_5)B_n^{\pm}$, $C_n^{\pm} = B_n^{\pm}(\gamma\exp(\pm a_5) - \cosh(\beta_n C))/\sinh(\beta_n C), a_5 = \alpha C\sin(\phi_0)$. Thus we have

$$Y_n^{\pm}(y) = \frac{B_n^{\pm}}{\sinh(\beta_n C)}F_n^{\pm}(y),$$

where $F_n^{\pm}(y) = \sinh(\beta_n(C-y)) + \gamma\exp(\pm a_5)\sinh(\beta_n y)$.

3.2 The solution of azymuthal velocity $U = U(x,y)$ and induced magnetic field $H = H(x,y)$

From Equations (2.1)–(2.2) it follows

$$U(x,y) = \frac{1}{2}(W_+(x,y)\exp(-\alpha(f_0(x,y)) - W_-(x,y)\exp(\alpha(f_0(x,y))),$$
$$H(x,y) = \frac{1}{2}(W_+(x,y)\exp(-\alpha(f_0(x,y)) + W_-(x,y)\exp(\alpha(f_0(x,y))).$$

Using Fourier series for functions $W_{\pm}(x,y)$ we obtain

$$U(x,y) = -\frac{I_0}{2L}\sum_{n=1}^{\infty}\frac{X_n}{\sinh(\beta_n C)(\lambda_n^2+a_6^2)}\big(F_n^+(y)(\exp(-A_{2,n}(x,y))(a_{3,n}-a_{4,n})$$
$$-\exp(-A_{1,n}(x,y))(a_{1,n}-a_{2,n}))$$
$$-F_n^-(y)(\exp(A_{2,n}(x,y))(-a_{3,n}-a_{4,n}) - \exp(A_{1,n}(x,y))(-a_{1,n}-a_{2,n}))\big),$$

where $A_{1,n}(x,y)=a_6(x+a)+b_1y$, $A_{2,n}(x,y)=a_6(x-a)+b_1y$, $b_1=\alpha\sin(\phi_0)$.

Therefore,

$$U(x,y)=\frac{I_0}{L}\sum_{n=1}^{\infty}\frac{s_{2,n}(x)}{s_{1,n}}(c_{1,n}(y)c_{0,n}(x,y)+\gamma c_{2,n}(y)c_{3,n}(x,y)),$$

where

$$\begin{aligned}
c_{0,n}(x,y)&=-a_{3,n}\cosh(A_{2,n}(x,y))-a_{4,n}\sinh(A_{2,n}(x,y))\\
&\quad+a_{1,n}\cosh(A_{1,n}(x,y))+a_{2,n}\sinh(A_{1,n}(x,y)),\\
c_{3,n}(x,y)&=-a_{3,n}\cosh(A_{2,n}(x,y)-a_5)-a_{4,n}\sinh(A_{2,n}(x,y)-a_5)\\
&\quad+a_{1,n}\cosh(A_{1,n}(x,y)-a_5)+a_{2,n}\sinh(A_{1,n}(x,y)-a_5),\\
c_{1,n}(y)&=\sinh(\beta_n(C-y)),c_{2,n}(y)=\sinh(\beta_n y),\\
s_{1,n}&=\sin(\beta_nC)(\lambda_n^2+a_6^2),s_{2,n}(x)=\sin(\lambda_n(x+L)).
\end{aligned}$$

Similarly, we obtain

$$H(x,y)=\frac{I_0}{L}\sum_{n=1}^{\infty}\frac{s_{2,n}(x)}{s_{1,n}}(c_{1,n}(y)c_{4,n}(x,y)+\gamma c_{2,n}(y)c_{5,n}(x,y)),$$

where

$$\begin{aligned}
c_{4,n}(x,y)&=a_{3,n}\sinh(A_{2,n}(x,y))+a_{4,n}\cosh(A_{2,n}(x,y))\\
&\quad-a_{1,n}\sinh(A_{1,n}(x,y))-a_{2,n}\cosh(A_{1,n}(x,y)),\\
c_{5,n}(x,y)&=a_{3,n}\sinh(A_{2,n}(x,y)-a_5)+a_{4,n}\cosh(A_{2,n}(x,y)-a_5)\\
&\quad-a_{1,n}\sinh(A_{1,n}(x,y)-a_5)-a_{2,n}\cosh(A_{1,n}(x,y)-a_5).
\end{aligned}$$

3.3 The solution of hydrodynamic flow rate U_q and magnetic flow rate H_q

Similarly, we can obtain the analytical expressions for hydrodynamic flow rate $U_q=\int_{-L}^{L}\int_0^C U(x,y)dxdy$, magnetic flow rate $H_q=\int_{-L}^{L}\int_0^C H(x,y)dxdy$. For hydrodynamic flow rate U_q we use the expression:

$$U_q=\frac{4}{L}(\sum_{i=1}^{N}(-1)^i(L_{4,i}-L_{5,i})(1-\gamma)),$$

where

$$\begin{aligned}
&L_{4,i}=L_{1,i}\,b_{3,i}\,b_{4,i}(a_6\,\sin(aL_{1,i})\,\cosh(a\,a_6)-L_{1,i}\,\cos(L_{1,i}a)\,\sinh(a\,a_6));\\
&L_{5,i}=L_{2,i}\,b_{8,i}\,b_{9,i}(a_6\,\cos(aL_{2,i})\,\sinh(a_6\,a)+L_{2,i}\,\sin(L_{2,i}a)\,\cosh(a_6\,a));\\
&b_{3,i}=b_1-b_{2,i}\sinh(a_5)/\sinh(Cb_{2,i});\ b_{4,i}=\frac{\sinh(La_6)}{(L_{1,i}^2+a_6^2)^3};\ L_{1,i}=\frac{i\pi}{L};\\
&b_{2,i}=\sqrt{\alpha^2+L_{1,i}^2};\ L_{2,i}=(2i-1)\pi/(2L);\ lb_{7,i}=\sqrt{\alpha^2+L_{2,i}^2};\\
&b_{8,i}=b_1-b_{7,i}\sinh(b_1C)/\sinh(Cb_{7,i});b_{9,i}=\frac{\cosh(a_6L)}{(L_{2,i}^2+a_6^2)^3}.
\end{aligned}$$

For magnetic flow rate H_q we obtain:

$$H_q = \frac{4}{L}(\sum_{i=1}^{N}(-1)^i\,(-L_{4,i} + L_{5,i})(1+\gamma)).$$

We use following formulas [1]:

$$\int \sinh(at+b)\sinh(ct+d)dt = \frac{0.5}{a+c}\sinh((a+c)t+b+d)$$
$$-\frac{0.5}{a-c}\sinh((a-c)t+b-d),\quad \int \sinh(at+b)\cosh(ct+d)dt$$
$$= \frac{0.5}{a+c}\cosh((a+c)t+b+d) + \frac{0.5}{a-c}\cosh((a-c)t+b-d),$$
$$\int \cosh(at+b)\cosh(ct+d)dt = \frac{0.5}{a+c}\sinh((a+c)t+b+d)$$
$$+\frac{0.5}{a-c}\sinh((a-c)t+b-d),\quad \int \cosh(at+b)\sin(ct+d)dt$$
$$= \frac{1}{a^2+c^2}(a\sin(ct+d)\sinh(at+b) - c\cosh(at+b)\cos(ct+b)),$$
$$\int \sinh(at+b)\sin(ct+d)dt = \frac{1}{a^2+c^2}(a\sin(ct+d)\cosh(at+b)$$
$$-c\sinh(at+b)\cos(ct+b)).$$

3.4 The solution of electric current densities J_x, J_y

Using the electric current densities $J_x = \frac{\partial H}{\partial y}, J_y = -\frac{\partial H}{\partial x}$, we obtain $\big(\frac{\partial A_1(x,y)}{\partial x} = \frac{\partial A_2(x,y)}{\partial x} = a_6, \frac{\partial A_1(x,y)}{\partial y} = \frac{\partial A_2(x,y)}{\partial y} = b_1\big)$:

$$J_y(x,y) = -\frac{I_0}{L}\sum_{n=1}^{\infty}\Big(\frac{s_{3,n}(x)}{s_{1,n}}\big(c_{1,n}(y)c_{4,n}(x,y) + \gamma c_{2,n}(y)c_{5,n}(x,y)\big)$$
$$+\frac{s_{2,n}(x)}{s_{1,n}}(c_{1,n}(y)c_{6,n}(x,y) + \gamma c_{2,n}(y)c_{7,n}(x,y))\Big),$$

where

$$s_{3,n}(x)=\lambda_n\cos(\lambda_n(x+L)),\ c_{6,n}(x,y)=\frac{\partial c_{4,n}(x,y)}{\partial x}=a_6(a_{3,n}\cosh(A_{2,n}(x,y))$$
$$+a_{4,n}\sinh(A_{2,n}(x,y)) - a_{1,n}\cosh(A_{1,n}(x,y)) - a_{2,n}\sinh(A_{1,n}(x,y))),$$
$$c_{7,n}(x,y)=\frac{\partial c_{5,n}(x,y)}{\partial x}=a_6(a_{3,n}\cosh(A_{2,n}(x,y)-a_5)+a_{4,n}\sinh(A_{2,n}(x,y)-a_5)$$
$$-a_{1,n}\cosh(A_{1,n}(x,y)-a_5) - a_{2,n}\sinh(A_{1,n}(x,y)-a_5)).$$

Similarly,

$$J_x(x,y) = \frac{I_0}{L}\sum_{n=1}^{\infty}\frac{s_{2,n}(x)}{s_{1,n}}(d_{1,n}(y)c_{4,n}(x,y) + \gamma d_{2,n}(y)c_{5,n}(x,y)$$
$$+c_{1,n}(y)c_{8,n}(x,y) + \gamma c_{2,n}(y)c_{9,n}(x,y)),$$

where

$$d_{1,n}(y) = -\beta_n cosh(\beta_n(C-y)),\ \ d_{2,n}(y) = \beta_n cosh(\beta_n y),$$
$$c_{8,n}(x,y)=\frac{\partial c_{4,n}(x,y)}{\partial y}=b_1(a_{3,n}\cosh(A_{2,n}(x,y)) + a_{4,n}\sinh(A_{2,n}(x,y))$$
$$- a_{1,n}\cosh(A_{1,n}(x,y)) - a_{2,n}\sinh(A_{1,n}(x,y))),$$
$$c_{9,n}(x,y)=\frac{\partial c_{5,n}(x,y)}{\partial y}=b_1(a_{3,n}\cosh(A_{2,n}(x,y)-a_5)+a_{4,n}\sinh(A_{2,n}(x,y)$$
$$- a_5) - a_{1,n}\cosh(A_{1,n}(x,y)-a_5) - a_{2,n}\sinh(A_{1,n}(x,y)-a_5)).$$

4 Some numerical results

We use following parameters [18]: $N = 240, L = 3.2, C = 4.8, a = 1, I_0 = 1$, $\gamma = 0; 1; -1$, $Ha = [1; 10; 30; 100]$ for $\phi_0 = \pi/2$ and $Ha = [1; 4; 8; 10]$ for $\phi_0 = \pi/4, \phi_0 = 0$. N is the number of terms of the Fourier series with maximal absolute errors: 6.10^{-19} $(Ha = 1)$ 2.10^{-18} $(Ha = 100)$.

The dimensionless values of U, H, J_y, J_x are represented for fixed $x = 0$ depend on y and $y = 1.2$ and $y = 3.6$ depend on x, all values are depending on Ha. Maximal value of flow rate U_q for $Ha = 100$, $\phi_0 = \pi/2$: $4.780(\gamma = 0)$, $9.560(\gamma = -1), 0(\gamma = 1)$; minimal value of magnetic flow rate:
$H_q = -4.760$ $(\gamma = 0), -9.560(\gamma = 1), 0(\gamma = -1)$.

The values corresponding for $\phi_0 = \pi/4, Ha = 10$ are the following:
$U_q = 3.068(\gamma = 0), 6.136(\gamma = -1), 0(\gamma = 1)$, $H_q = -3.068(\gamma = 0)$, $-6.136(\gamma = 1), 0(\gamma = -1)$. If $\phi_0 = 0$, then $U_q = H_q = 0$.

4.1 A transverse uniform magnetic field $\phi_0 = \pi/2$

For $\gamma = 0; -1$ the velocity profiles shown in Figures 4–5 and the velocity distribution in Figure 6 demonstrate a flow concentration in area between electrodes with increasing the Hartmann number.

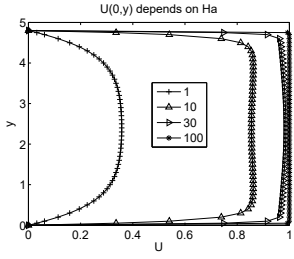

Figure 4. Velocity profiles $U(0, y)$ depends on Ha for $\gamma = -1$.

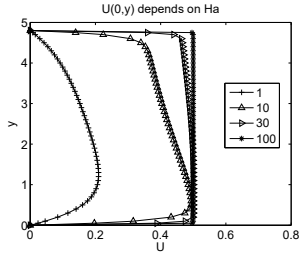

Figure 5. Velocity profiles $U(0, y)$ depends on Ha for $\gamma = 0$.

With growing Ha, the flow gets narrower and tends to be equal in width to the distance between the electrodes. For $\gamma = -1$, the flow rapidly homogenizes over the field with an increase in the Hartmann number (Figure 4). In this

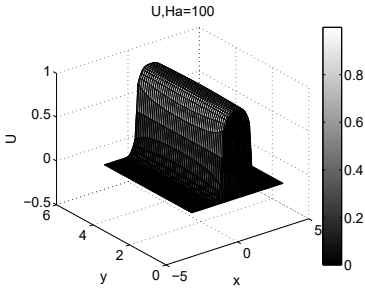

Figure 6. Velocity U distribution for $Ha = 100$, $\gamma = -1$.

case, one can clearly see a decrease in the thickness of the Hartmann layers (proportional to Ha^{-1}) with increasing the field.

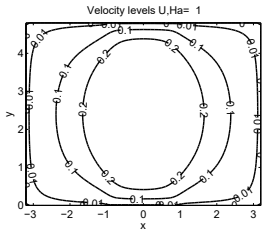

Figure 7. Isolines of velocity by $Ha = 1$ for $\gamma = -1$.

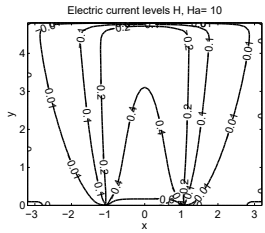

Figure 8. Levels of electric current by $Ha = 10$ for $\gamma = 0$.

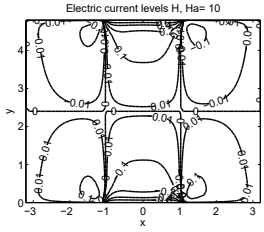

Figure 9. Levels of electric current by $Ha = 10$ for $\gamma = -1$.

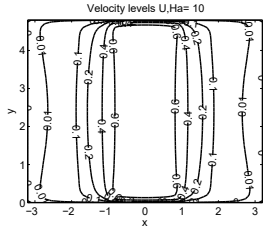

Figure 10. Isolines of velocity by $Ha = 10$ for $\gamma = -1$.

The isolines of velocity and levels of electric current in the cross section of the duct shown in Figures 7–10 and current density Jx levels (Figure 11) demonstrate the concentration of the flow in the lower and upper half of the duct, where the electrodes are located and non-uniform distribution of the electric current along the field.

For $\gamma = 1$, the velocity profiles shown in Figure 12 indicate a decrease in velocity in the central region of the flow with an increase in Ha. We can definitely say that at the height $y = C/2$ and on the channel walls $y = 0, y = C$ the velocity is equal to zero. However, in the regions $0 < y < C/2$ and $C/2 < y < C$ at $Ha = 100$, the velocities have a small but non-zero value and are oppositely directed.

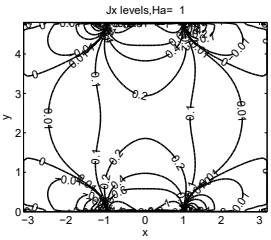

Figure 11. Levels of electric current density Jx by $Ha = 1$ for $\gamma = -1$.

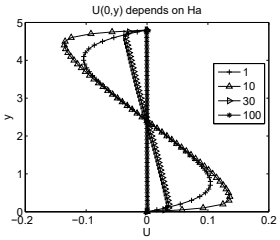

Figure 12. Velocity profiles $U(0, y)$ depends on Ha for $\gamma = 1$.

Velocity surfaces (distribution) at $Ha = 100$ in the section (x, y) we can see in Figure 13, magnetic field distribution in Figure 14 and the isolines of velocity and levels of electric current for $Ha = 10$ in Figures 15,16.

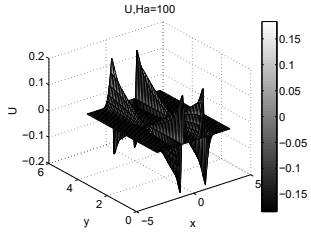

Figure 13. Velocity U distribution for $Ha = 100$, $\gamma = 1$.

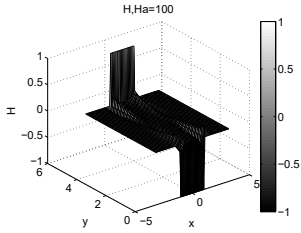

Figure 14. Magnetic field H distribution for $Ha = 100$, $\gamma = -1$.

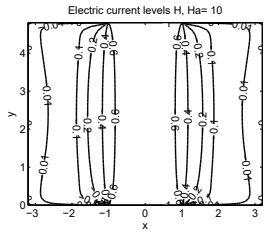

Figure 15. Levels of electric current by $Ha = 10$ for $\gamma = 1$.

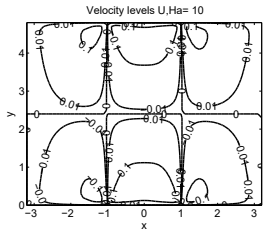

Figure 16. Isolines of velocity by $Ha = 10$ for $\gamma = 1$.

The levels of electric current density Jy by $Ha = 1$ for $\gamma = 1; -1$ are shown in Figures 17–18.

4.2 An oblique transverse uniform magnetic field $\phi_0 = \pi/4$

At $\gamma = 0$, the velocity profiles depend on Ha deformed by an inclined magnetic field is observed (Figure 19), where with an increase in Ha numbers if in the lower part of the section the velocity increases monotonically, then in the upper part of the section the velocity decreases.

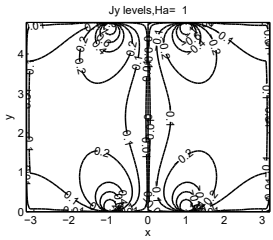

Figure 17. Levels of electric current density Jy by $Ha = 1$ for $\gamma = 1$.

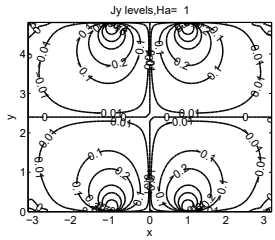

Figure 18. Levels of electric current density Jy by $Ha = 1$ for $\gamma = -1$.

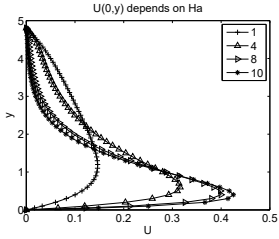

Figure 19. Velocity profiles $U(0, y)$ depends on Ha for $\gamma = 0$.

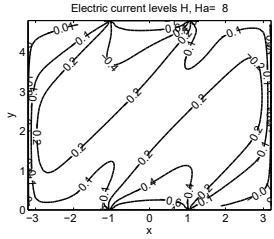

Figure 20. Levels of electric current by $Ha = 8$ for $\gamma = 1$.

For $Ha = 8$ (different γ) two oblique flows arise, they are shown in Figures 21–23, the corresponding distribution of electric currents is shown in Figure 20.

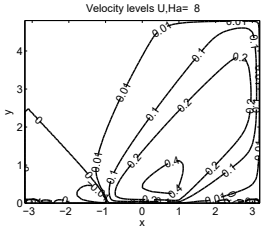

Figure 21. Isolines of velocity by $Ha = 8$ for $\gamma = 0$.

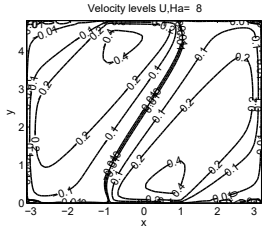

Figure 22. Isolines of velocity by $Ha = 8$ for $\gamma = 1$.

The velocity isolines shown in Figure 21 for $\gamma = 0$ indicate that the flow tends to orient itself along the magnetic field lines due to the action of the asymmetric distribution of the Lorentz forces. In this case, a weak reverse flow is observed on the left.

The velocity isolines shown in Figure 22 for $\gamma = 1$ indicate that two fields of oppositely directed velocities over cross section demonstrate a turn and an orientation of flows along the magnetic field lines.

A transverse shear layer appears between the flows, stretched along the lines of the magnetic field in thickness proportional to $1/Ha^{0.5}$ [9].

The velocity isolines shown in Figure 23 for $\gamma = -1$ demonstrate two max-

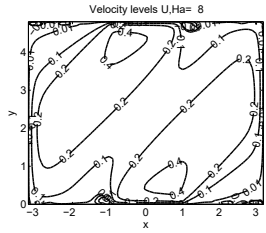

Figure 23. Isolines of velocity by $Ha = 8$ for $\gamma = -1$.

imal values of velocity in cross section. The distributions of the components J_x and J_y are fully consistent with behaviour of the induced magnetic fields along the $x-$ and $y-$ coordinates displayed in Figure 20 since their values are defined by $J_x = \frac{\partial H}{\partial y}, J_y = -\frac{\partial H}{\partial x}$.

We observe a structure consisting of two flows deformed by an inclined magnetic field. With an appropriate levels of electric currents density J_y in Figures 24–25 for $Ha = 1$ is observed, tending to be parallel to the magnetic field.

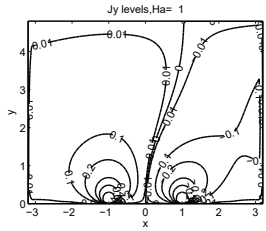

Figure 24. Levels of electric current density Jy by $Ha = 1$ for $\gamma = 0$.

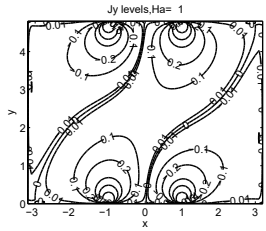

Figure 25. Levels of electric current density Jy by $Ha = 1$ for $\gamma = -1$.

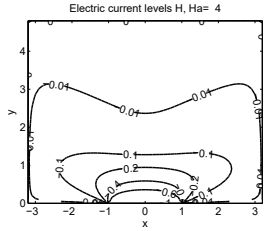

Figure 26. Levels of electric current by $Ha = 4$ for $\gamma = 0$.

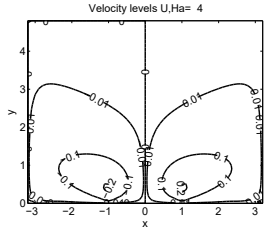

Figure 27. Isolines of velocity by $Ha = 4$ for $\gamma = 0$.

4.3 An uniform magnetic field is parallel to the walls $\phi_0 = 0$

At $\gamma = 0$ for $Ha = 4$ two flows appear on the left and on the right are observed (Figure 27) (for $\gamma = 1$, $Ha = 1$, see Figure 28).

The distribution of electric currents, shown in Figure 26, corresponds to these flows, since the current components Jy, interacting with field, have accordant direction in the channel section on the left and on the right.

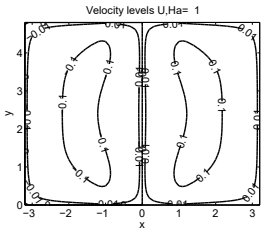

Figure 28. Isolines of velocity by $Ha = 1$ for $\gamma = 1$.

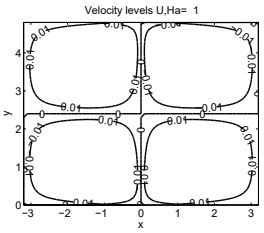

Figure 29. Isolines of velocity by $Ha = 1$ for $\gamma = -1$.

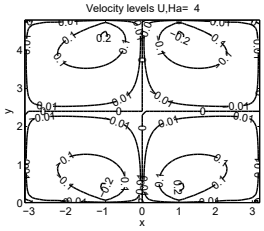

Figure 30. Isolines of velocity by $Ha = 4$ for $\gamma = -1$.

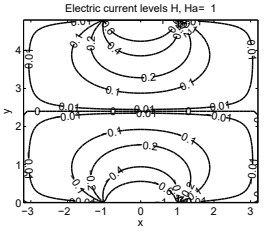

Figure 31. Levels of electric current by $Ha = 1$ for $\gamma = -1$.

At $\gamma = -1$ four flows are realized (Figures 27, 29, 30) corresponding to the electric current distribution shown in Figure 31. At $\gamma = 1$ in Figure 32 we can see the levels of electric current density Jx by $Ha = 1$.

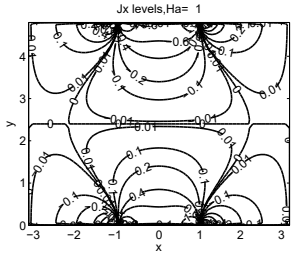

Figure 32. Levels of electric current density Jx by $Ha = 1$ for $\gamma = 1$.

5 Conclusions

1. We have obtained analytical solutions and computed the plane free shear flows of conducting fluid in a rectangular duct.

2. The differential problem is solved analytically using Fourier method and numerically using Matlab.

3. We investigated steady flows for three types of the current injection depending on a parameter γ and on magnetic field directions at an angle ϕ_0.

4. In the first case, by one couple of the linear electrodes, $\gamma = 0$, in the second case, by two couples of electrodes with electric currents in areas between electrodes in the same direction $\gamma = -1$ and in the third case, by two couples of electrodes with currents in areas between electrodes in opposite directions $\gamma = 1$.

5. The results of the numerical experiments can give some new physical conclusions about the MHD flow, generated as a result of the interaction of the electric current injected into the liquid.

References

[1] M. Abramovith and U. Stigan. *Handbook of mathematical functions with formulas, graphs and mathematical tables.* National Bureau of Standards Applied mathematical series-55, 1964.

[2] K.P. Acosta-Zamora and A. Beltran. Numerical study of the induced electric current of electrovortex flow in a cuboid vessel. *Magnetohydrodynamics*, **58**(1-2):115–124, 2022. https://doi.org/10.22364/mhd.58.1-2.12.

[3] Th. Arlt and L. Buhler. Numerical simulation of time-depending hunt flows with inite wall conductivity. *Magnetohydrodynamics*, **55**(3):319–336, 2019. https://doi.org/10.22364/mhd.55.3.5.

[4] L. Bougoffa, S. Mziou and R.C. Rach. Exact and approximate analytic solutions of the Jeffery-Hamel flow problem by the Duan-Rach modified a domain decomposition method. *Mathematical Modelling and Analysis*, **21**(2):174–187, 2016. https://doi.org/10.3846/13926292.2016.1145152.

[5] A. Buikis, L. Buligins and H. Kalis. Mathematical modelling of alternating electromagnetic and hydrodynamic fields induced by bar type conductors in a cylinder. *Mathematical Modelling and Analysis*, **14**(1):1–9, 2009. https://doi.org/10.3846/1392-6292.2009.14.1-9.

[6] A. Buikis and H. Kalis. Numerical modelling of heat and magnetohydrodynamic flows in a finite cylinder. *Computational Methods in Applied Mathematics*, **2**(3):243–259, 2002. https://doi.org/10.2478/cmam-2002-0015.

[7] A. Buikis, H. Kalis and A. Gedroics. Mathematical model of 2-d magnetic and temperature fields induced by alternating current feeding the bar conductors in cylinder. *Magnetohydrodynamics*, **46**(1):41–58, 2010. https://doi.org/10.22364/mhd.46.1.4.

[8] A. Gedroics and H. Kalis. Mathematical modelling of 2-D magnetohydrodynamic flow between two coaxial cylinders in an external magnetic field. *Magnetohydrodynamics*, **46**(2):153–170, 2010. https://doi.org/10.22364/mhd.46.2.4.

[9] J.C.R. Hunt and D.G. Malcolm. Some electrically driven flows in magnetohydrodynamics. Part 2. Theory and experiment. *Journal of Fluid Mechanics*, **33**(4):775–801, 1968. https://doi.org/10.1017/S0022112068001679.

[10] J.C.R. Hunt and W.E. Williams. Some electrically driven flows in magnetohydrodynamics. Part 1. Theory. *Journal of Fluid Mechanics*, **31**(4):705–772, 1968. https://doi.org/10.1017/S002211206800042X.

[11] H. Kalis and I. Kangro. *Effective finite difference and Conservative Averaging methods for solving problems of mathematical physics*. Rezekne Academy of Technologies, Rezekne, 2021.

[12] H. Kalis and Yu. Kolesnikov. Electrically driven free shear flow in a duct under a transverse uniform magnetic field. *Magnetohydrodynamics*, **59**(1):3–22, 2023.

[13] H. Kalis and M. Marinaki. Numerical study of 2-d MHD convection around periodically placed cylinders. *International Journal of Pure and Applied Mathematics*, **110**(3):503–517, 2016. https://doi.org/10.12732/ijpam.v110i3.10.

[14] H. Kalis, M. Marinaki and A. Gedroics. Mathematical modelling of 2-d MHD flow around infinite cylinders with square-section placed periodically. *Magnetohydrodynamics*, **48**(3):527–542, 2012. https://doi.org/10.22364/mhd.48.3.6.

[15] K.E. Kalis. Plane-parallel free flow of a conducting fluid with rectilinear current lines in a strong homogeneous magnetic field. *Magnetohydrodynamics*, **14**(2):65–72, 1978. Translated from Magnitnaya Gidrodinamika.

[16] Kh.E. Kalis. Time-depending deformation of three-dimensional perturbations in a current of viscous conductive liquid in a strong uniform magnetic field. *Magnetohydrodynamics*, **16**(4):352–356, 1980.

[17] Kh.E. Kalis. Special computational methods for the solution of MHD problems. *Magnetohydrodynamics*, **30**(2):119–129, 1994.

[18] Kh.E. Kalis and Y.B. Kolesnikov. Influence on a homogeneous transverse magnetic field on shear flow of a viscous electically conducting fluid. *Magnetohydrodynamics*, **5**(2):51–54, 1979. Translated from Magnitnaya Gidrodinamika.

[19] Kh.E. Kalis and Yu.B. Kolesnikov. A single vortex in a homogenous axial magnetic field with velocity component along the field. *Magnetohydrodynamics*, **17**(1):26–31, 1981. Translated from Magnitnaya Gidrodinamika.

[20] Kh.E. Kalis and Yu.B. Kolesnikov. Plane-parallel shear flow un a transverse magnetic field. *Magnetohydrodynamics*, **20**(1):57–60, 1984.

[21] A.A. Klyukin, Yu.B. Kolesnikov and V.B. Levin. Experimental investigation of a free rotating layer in an axial magnetic field. i - Stable conditions. *Magnetohydrodynamics*, **16**(1):75–79, 1980.

[22] Yu. Kolesnikov and H.Kalis. Electrically driven plane free shear flow in a duct under an oblique transverse uniform magnetic field. *Magnetohydrodynamics*, **59**(2):119–134, 2023.

[23] Yu. Kolesnikov and H. Kalis. Electrically driven cylindrical free shear flows under an axial uniform magnetic field. *Magnetohydrodynamics*, **57**(2):229–249, 2021. https://doi.org/10.22364/mhd.57.2.8.

[24] G. Korn and T. Korn. *Mathematical Handbook for scientists and engineers*. New York, Toronto London, 1961.

[25] H.K. Moffatt. Electrically driven steady flows in magnetohydrodynamics. *Proceedings of the 11th International Congress of Applied Mechanics*, pp. 946–953, 1964. https://doi.org/10.1007/978-3-662-29364-5_125.

[26] P.P. Vieweg, Yu. Kolesnikov and Ch. Karcher. Experimental study of a liquid metal film flow in a streamwise magnetic field. *Magnetohydrodynamics*, **58**(1-2):5–12, 2022. https://doi.org/10.22364/mhd.58.1-2.1.